

COMPARISONS OF THE SOLUTIONS FOR THE CATEGORY 3—PROBLEM 2: CASCADE—GUST INTERACTION

Edmane Envia

National Aeronautics and Space Administration
Glenn Research Center
Cleveland, Ohio 44135

Six different solutions were submitted for this benchmark problem. These were obtained using a variety of methods that can be conveniently categorized in two main groups, a nonlinear time-domain group and a linearized frequency-domain group. The first includes solutions submitted by (1) Hixon, (2) Nallasamy et. al, (3) Shieh et. al, and (4) Wang et. al, and the second includes solutions submitted by (5) Coupland and (6) Serrano et. al. Methods (1) and (2) use sixth order compact differencing schemes and the rest are essentially second order in space. With the exception of the solution submitted by Shieh et. al, all are individually discussed in great detail in the workshop proceedings. Comparisons of the submitted solutions with the benchmark solution are presented below. Due to differences in the level of solution detail provided to the author by the participants, the comparisons do not always include results from all submissions.

It should be noted at the outset that, since the benchmark solution itself was numerically computed, the comparisons are somewhat subjective. In order to provide maximum latitude for the participants of the workshop, no restrictions were placed on the type of method that could be used to solve the problem. Neither was there were any stipulations to use a particular grid topology or grid density. Therefore, without a detailed study of the critical features of the computed solutions, it is not possible to make concrete statements about the relative merits of one method over another. Such a study is beyond the scope of the current exercise, especially since complete flowfield details were not provided to the author by all participants. Instead a package, containing the information about the benchmark solution (both the steady and unsteady parts of it), is included on the proceedings' CD should the authors who submitted solutions for this problem wish to examine in detail the benchmark solution and compare their results to it.

The computed sound pressure levels (SPL) on the vane surface are presented in Figures 1 through 6. While there is some variation in the results, the agreement for the first two harmonic levels is quite good. The computed levels for the third harmonic show larger scatter probably as a result of differences in grid resolution among other factors. Another general observation is that the levels computed by the two high-order codes tend to be slightly higher than the ones calculated by the second order codes.

Figures 7 through 12 summarize the comparisons at the inflow and outflow planes. Here the agreement is not as good as that for the vane surface pressure results. The discrepancy may be related to the different implementations of the non-reflecting boundary conditions in these codes. Also, the perturbation levels at the inflow and outflow boundaries are at least one order of magnitude smaller the vane surface pressures making them more difficult to capture accurately. Here once again, the two high-order codes predict somewhat higher pressure levels.

In Figure 13, a comparison is shown between the computed results at $x = 0.00$ for frequency 2ω . This is a repeat of some of earlier results but is presented to accommodate the solution by submitted by Shieh et. al who had supplied only a limited set of results and, as a result, could not be included in the previous Figures.

Finally, the acoustic mode levels at the each of the three frequencies are shown at the inflow and outflow planes in Figures 14 through 16. All submitted solutions show the same mix of modes, but there are noticeable differences in the associated levels. Obviously these differences are related to those observed in Figures 7 through 12. Taken together these results suggest that the acoustic pressure levels on the vane are better captured than the radiated field. Among possible reasons for the discrepancies in the radiated levels are difference in the way different schemes handle the propagation of disturbances, and, of course, differences in the implementation of the non-reflecting boundary conditions.

It should be noted that this was the first attempt at solving a non-trivial cascade response problem for realistic frequencies of engineering interest. As a result, the comparisons should be viewed as encouraging in spite the differences, and the results of this study should serve as a stimulus to further investigate the similarity and differences between the various methods.

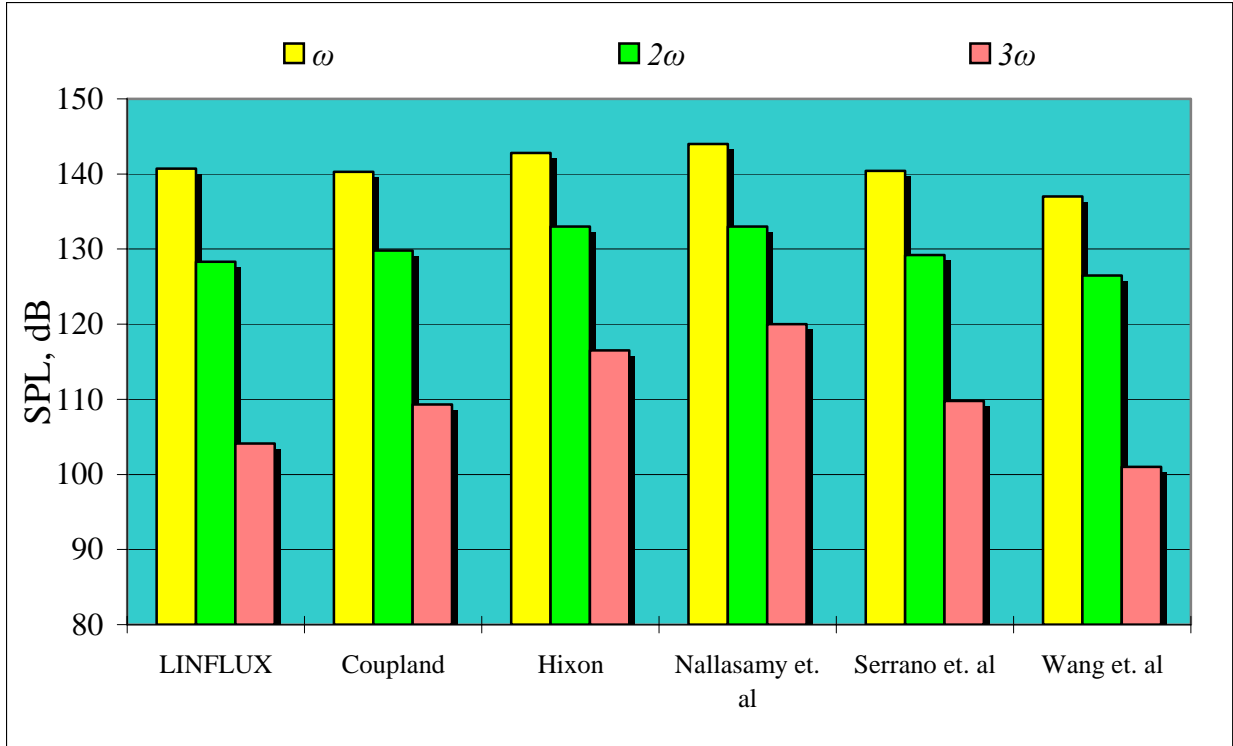


Figure 1. Comparison of computed sound pressure levels on the suction side of the vane at $x/c = -0.25$.

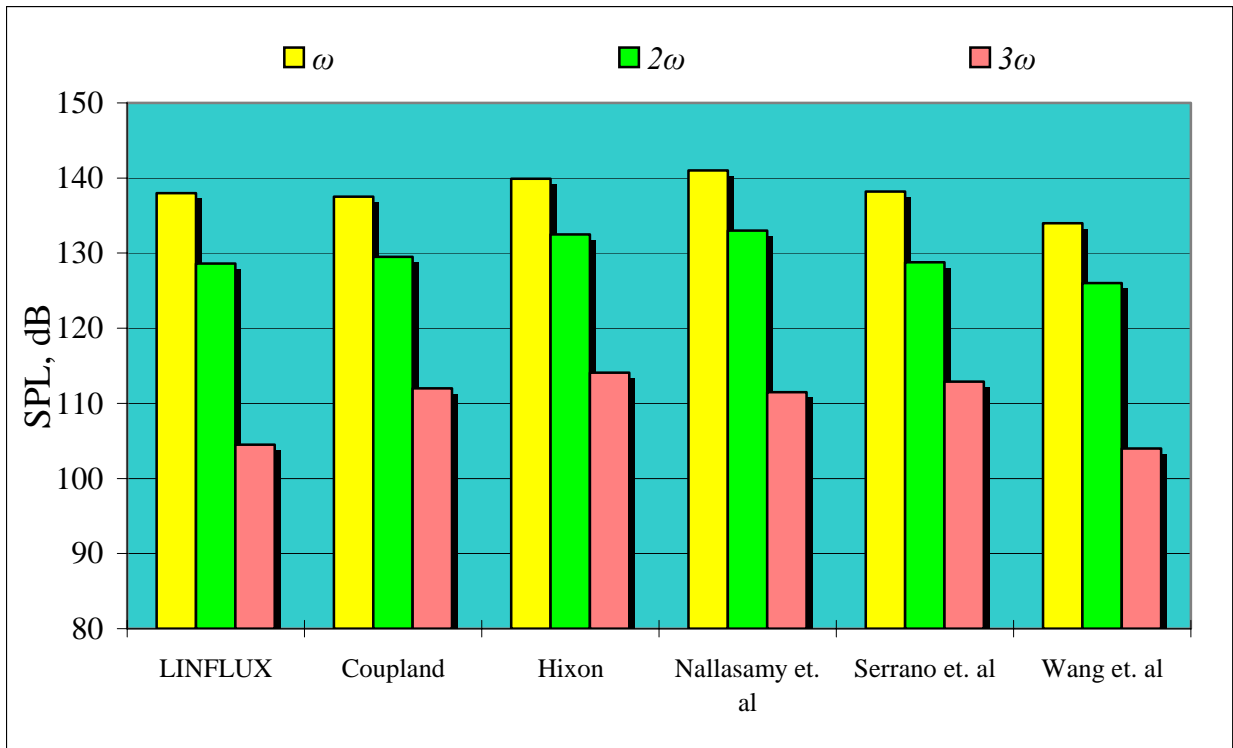


Figure 2. Comparison of computed sound pressure levels on the pressure side of the vane at $x/c = -0.25$.

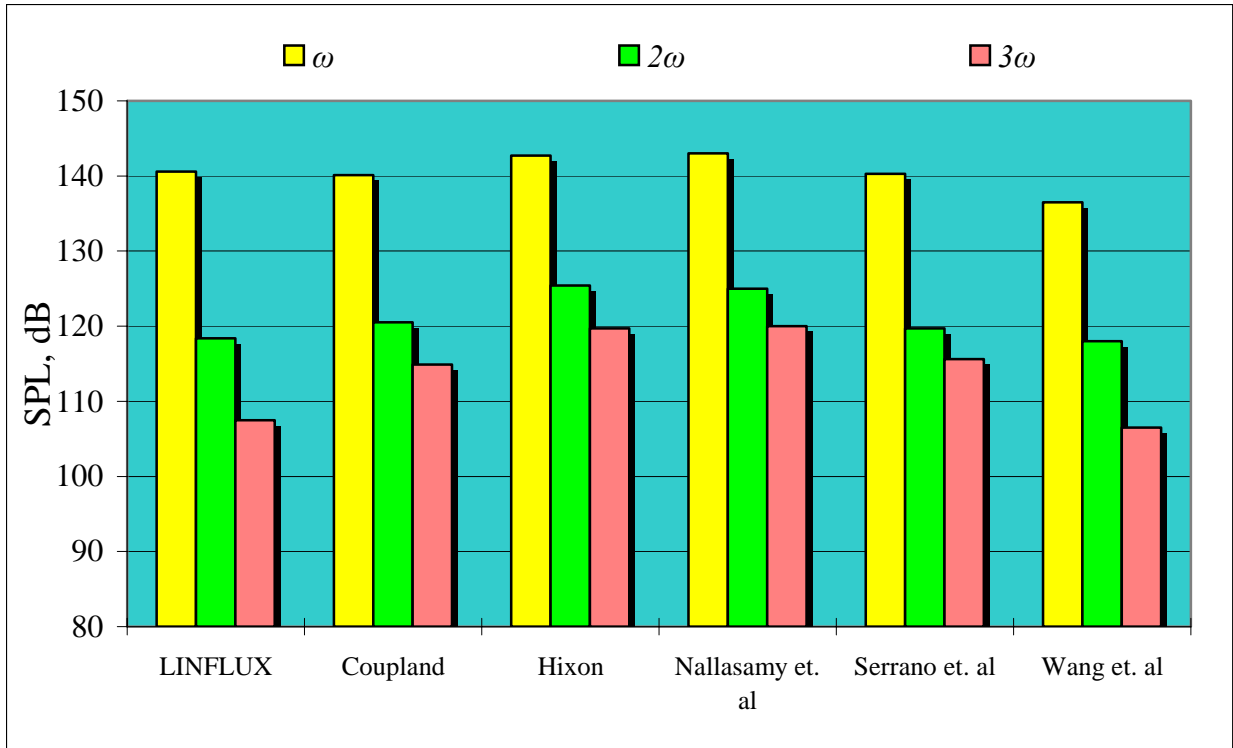


Figure 3. Comparison of computed sound pressure levels on the suction side of the vane at $x/c = 0.00$.

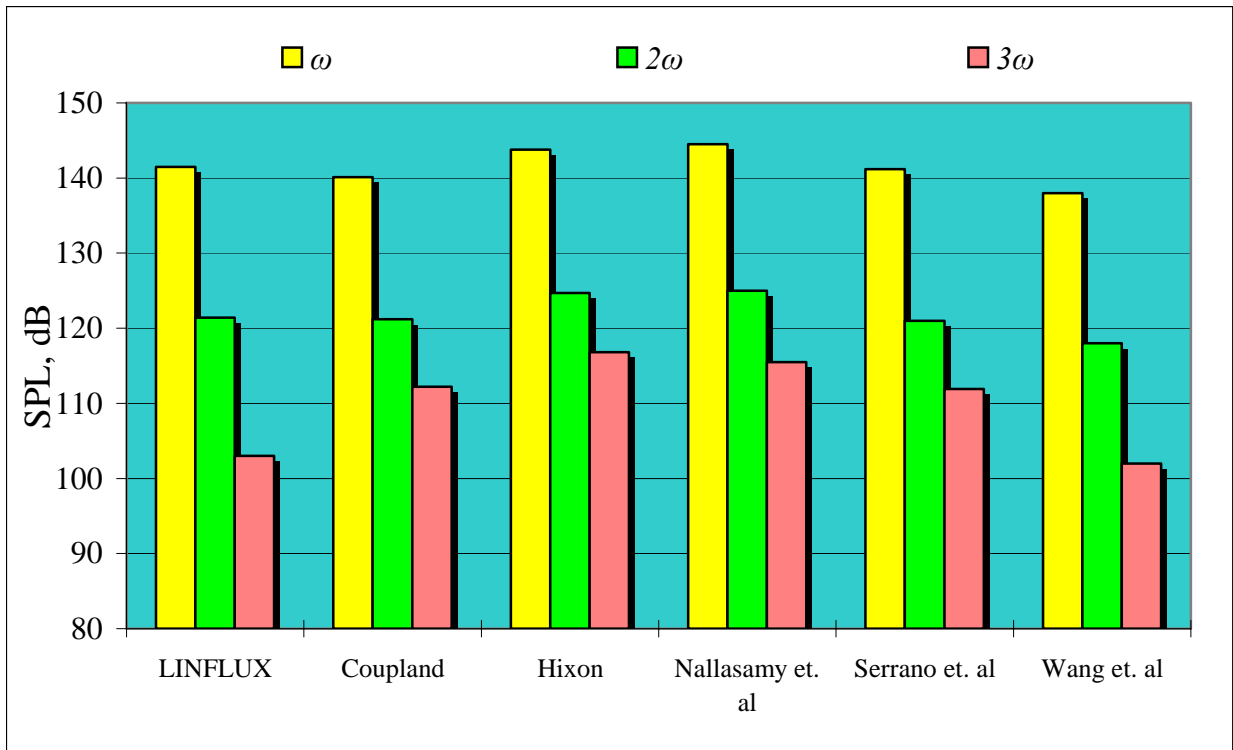


Figure 4. Comparison of computed sound pressure levels on the pressure side of the vane at $x/c = 0.00$.

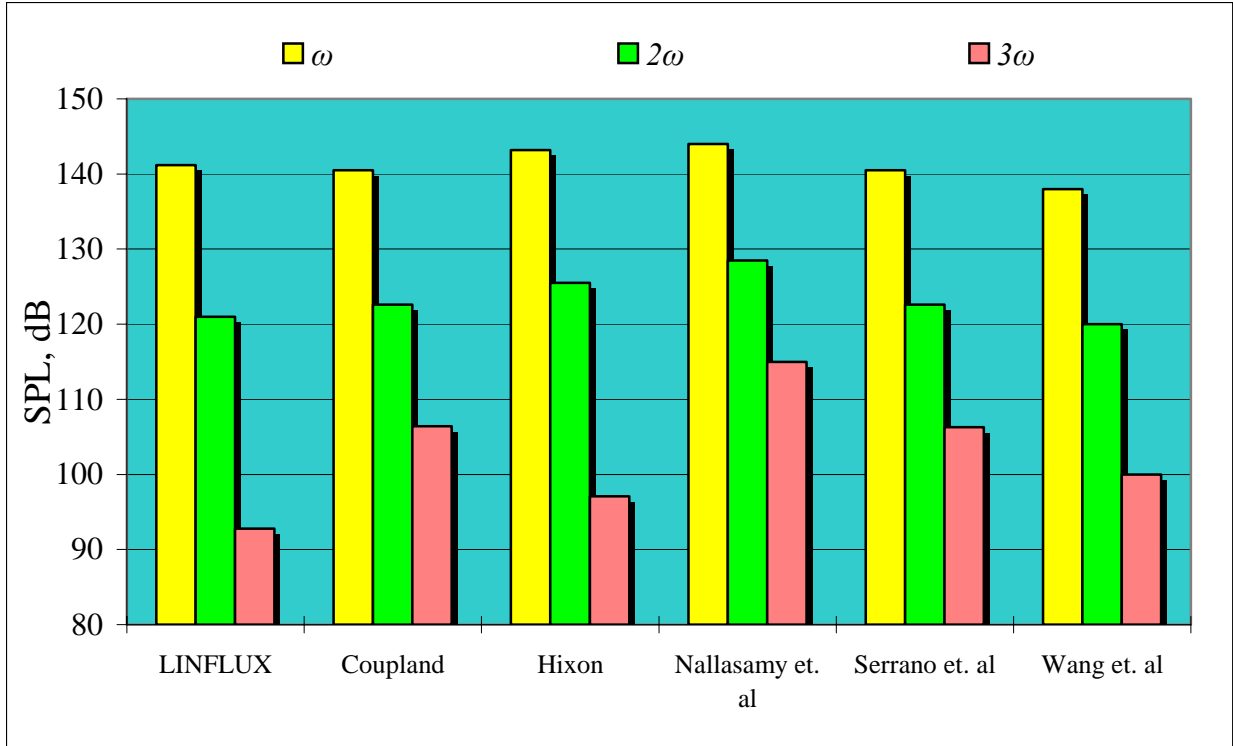


Figure 5. Comparison of computed sound pressure levels on the suction side of the vane at $x/c = +0.25$.

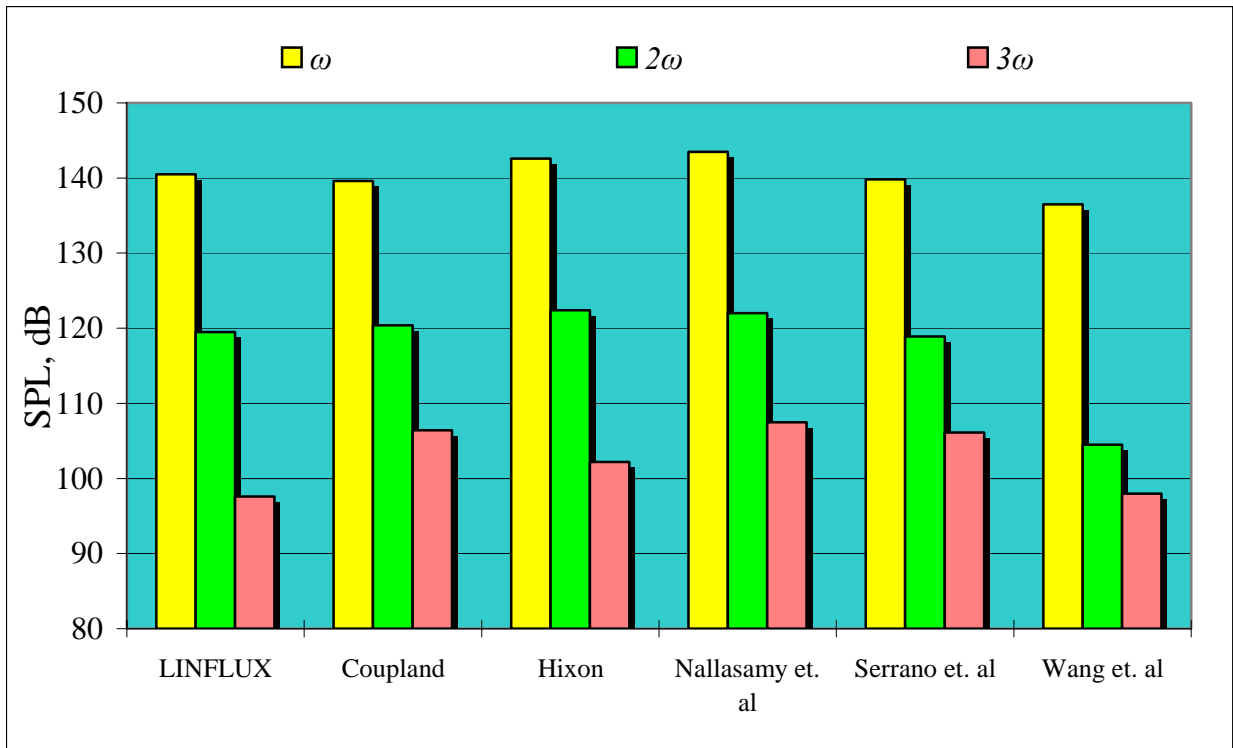


Figure 6. Comparison of computed sound pressure levels on the pressure side of the vane at $x/c = +0.25$.

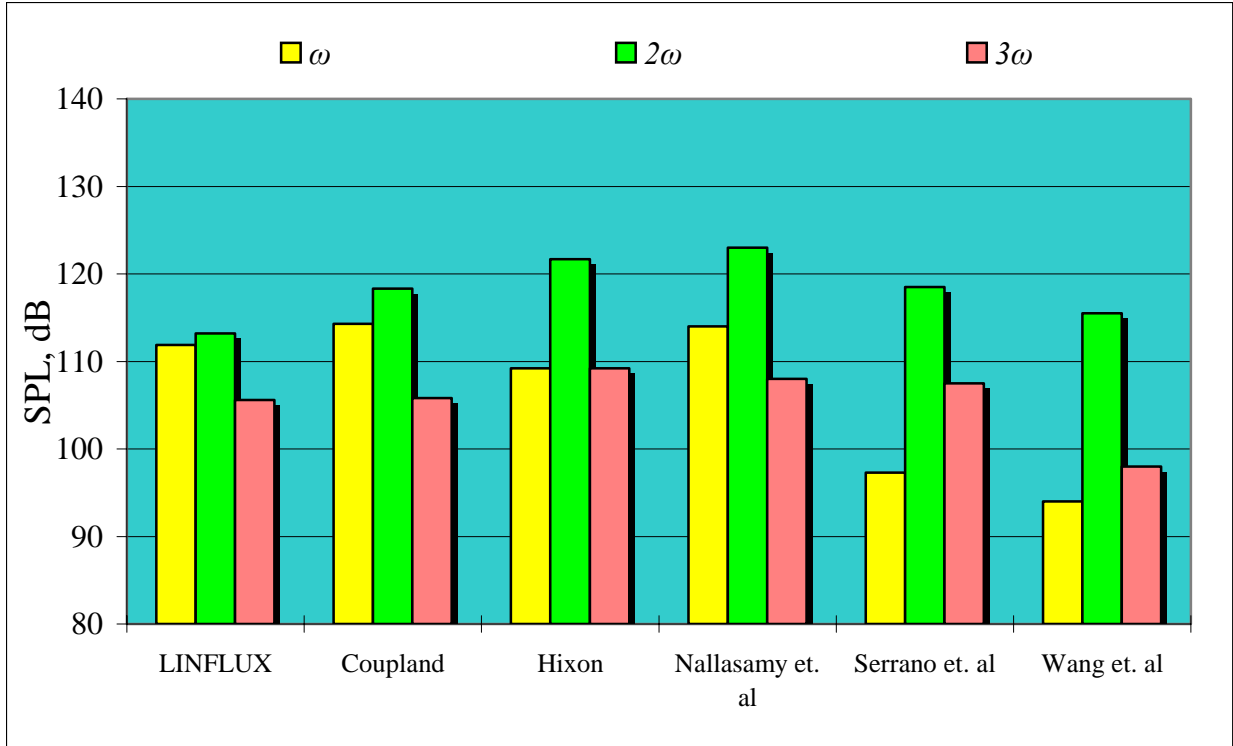


Figure 7. Comparison of computed sound pressure levels at the inflow plane at $y/c = -0.3$.

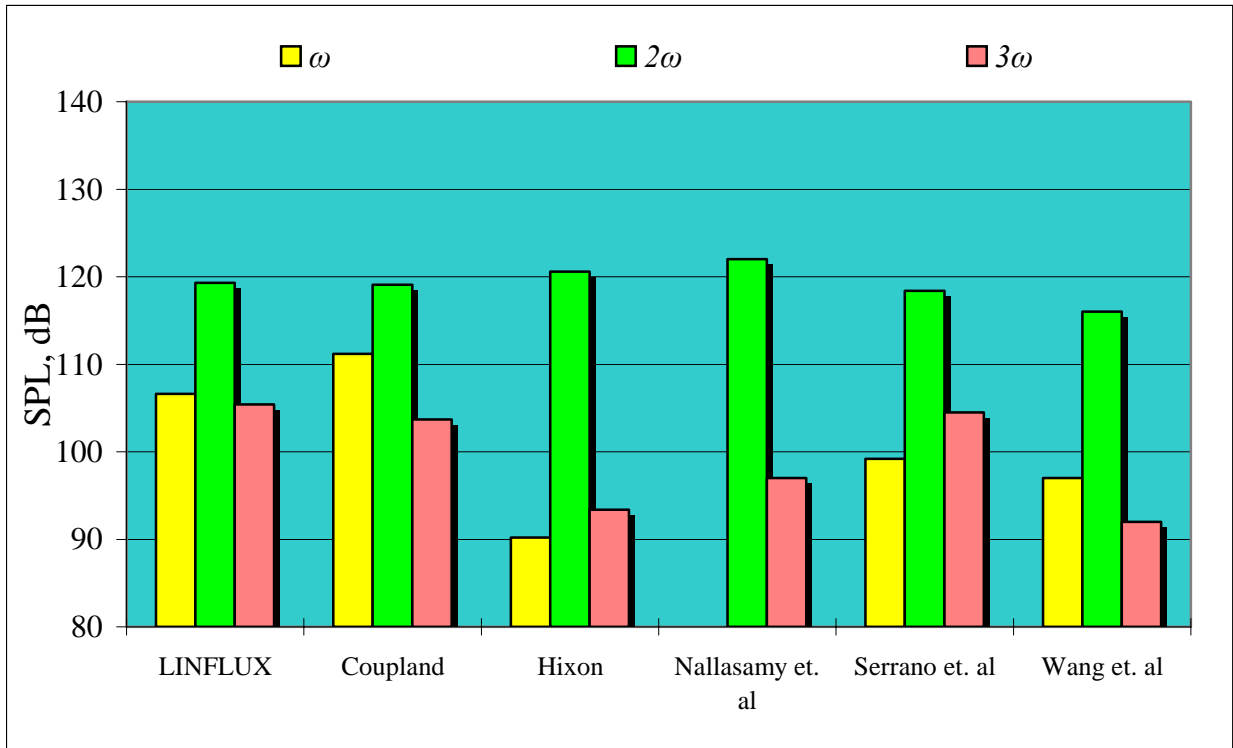


Figure 8. Comparison of computed sound pressure levels at the inflow plane at $y/c = 0.0$.

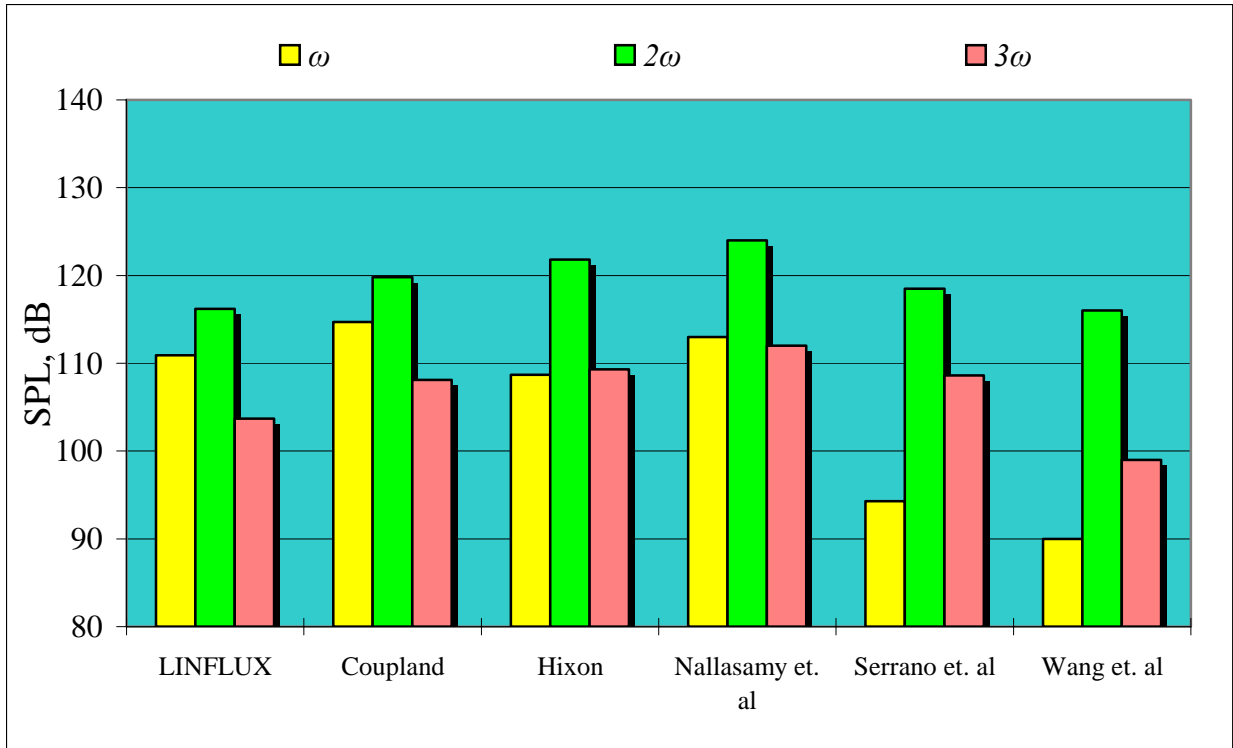


Figure 9. Comparison of computed sound pressure levels at the inflow plane at $y/c = +0.3$.

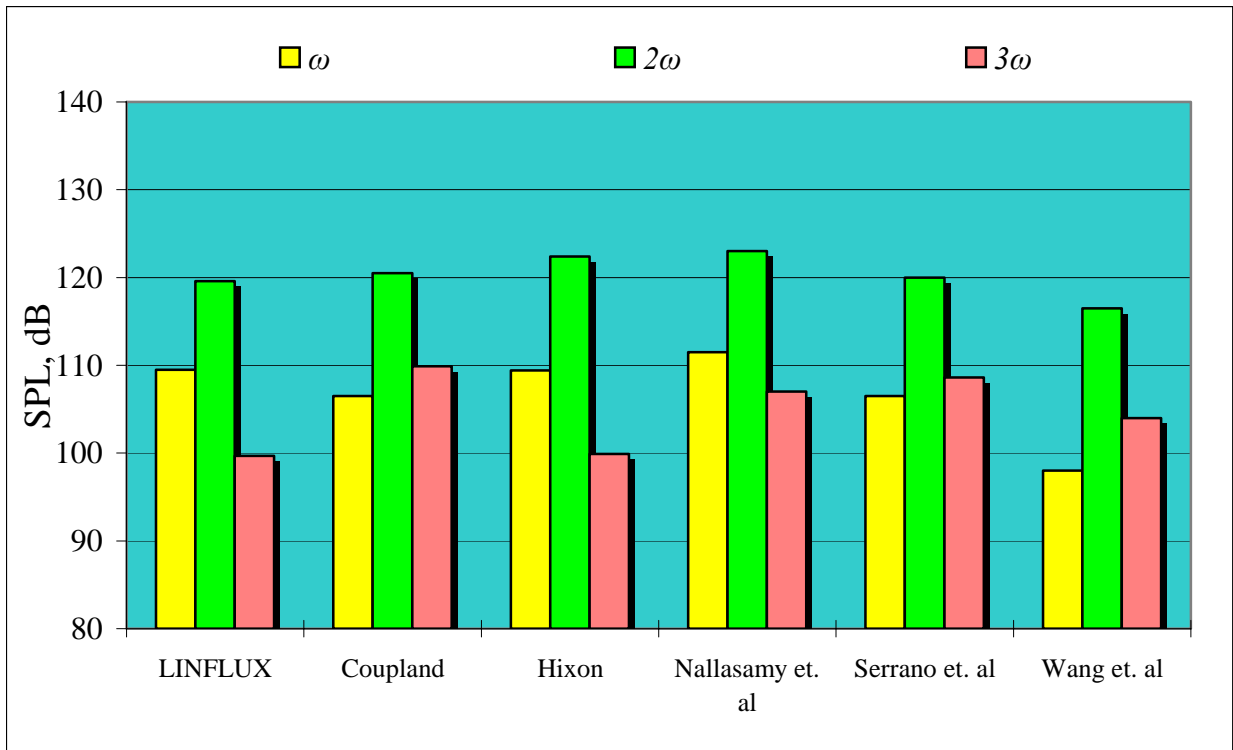


Figure 10. Comparison of computed sound pressure levels at the outflow plane at $y/c = -0.3$.

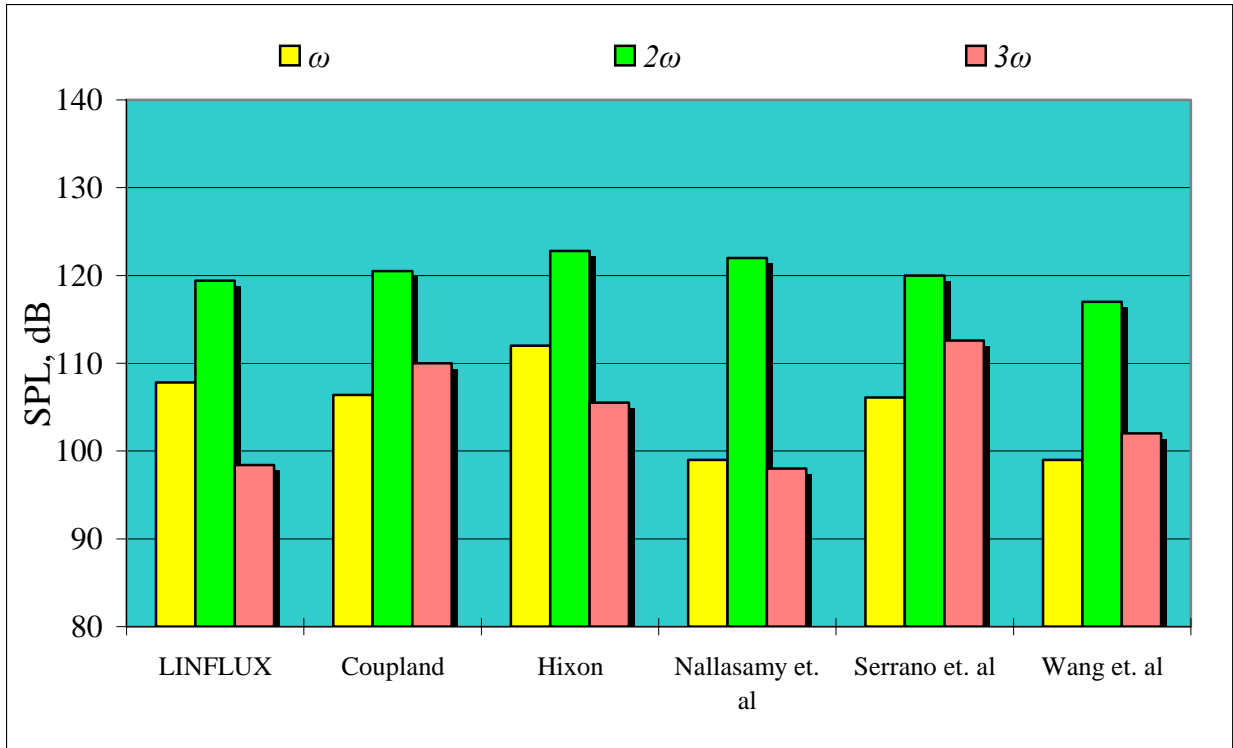


Figure 11. Comparison of computed sound pressure levels at the outflow plane at $y/c = 0.0$.

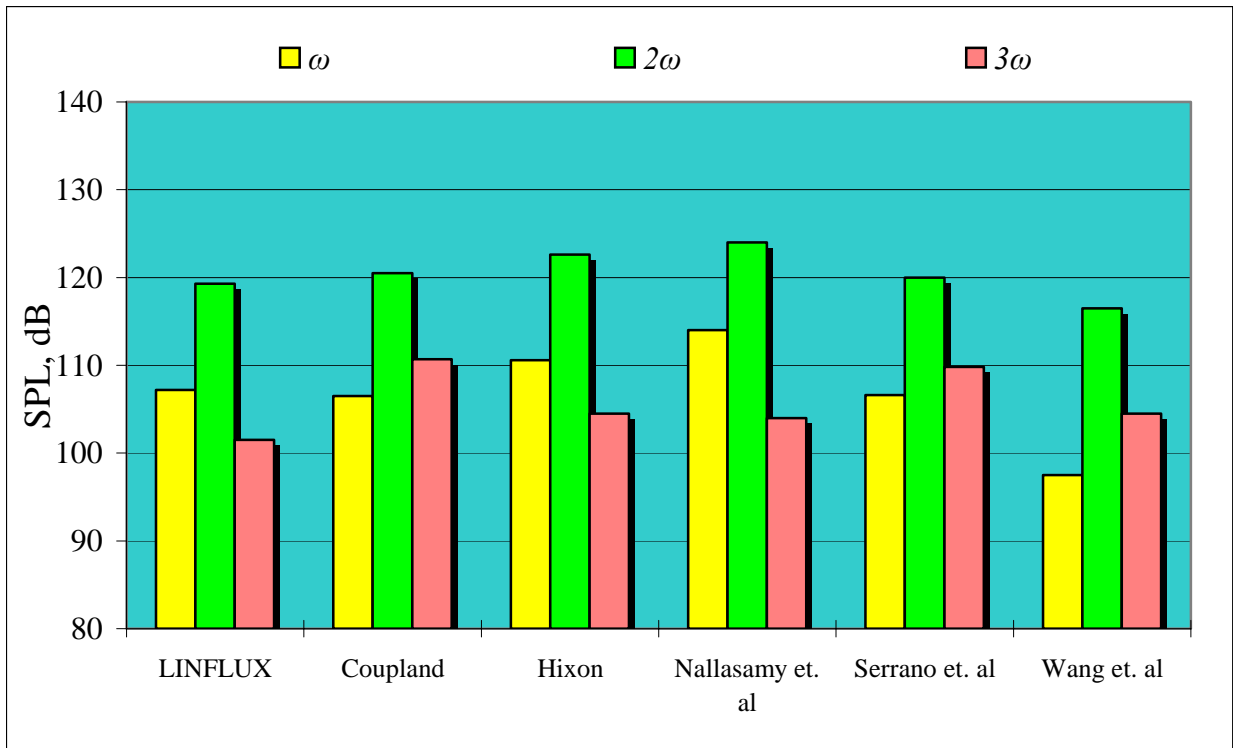


Figure 12. Comparison of computed sound pressure levels at the outflow plane at $y/c = +0.3$.

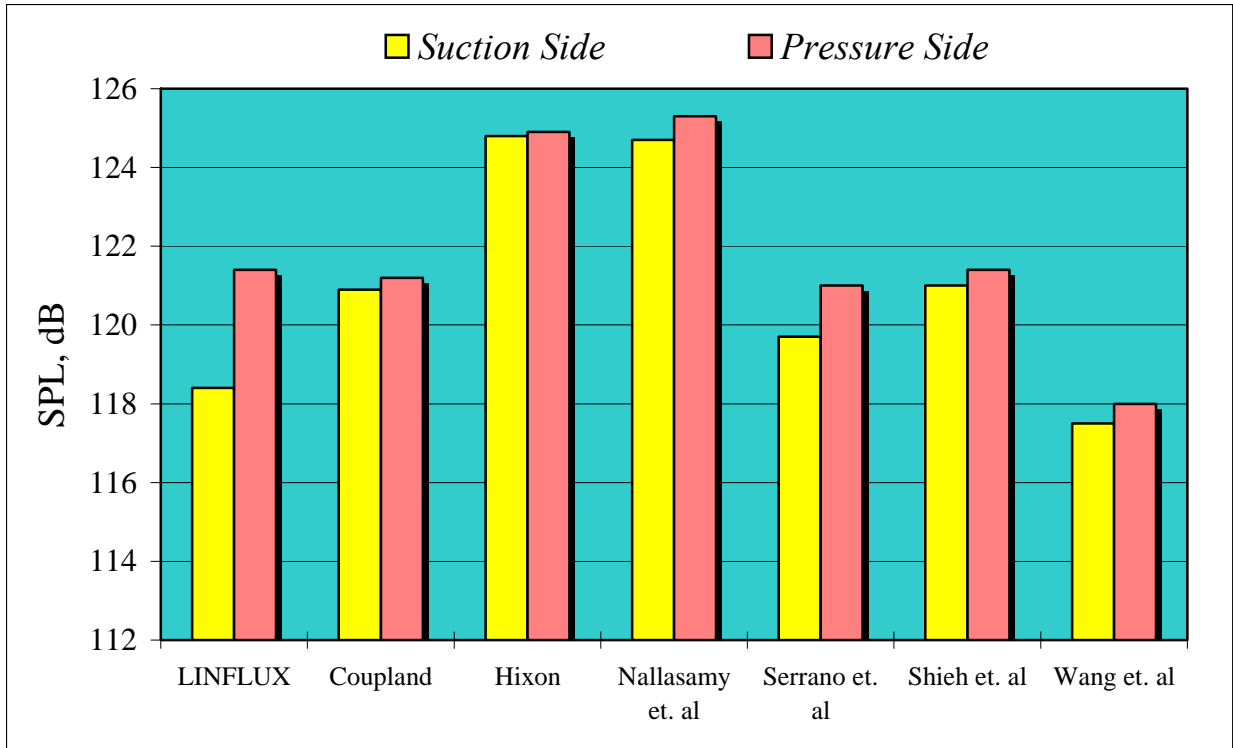


Figure 13. Comparison of computed sound pressure levels on the vane surface at $x/c = 0$ for frequency 2ω . (This chart includes results from Shieh et. al submission.)

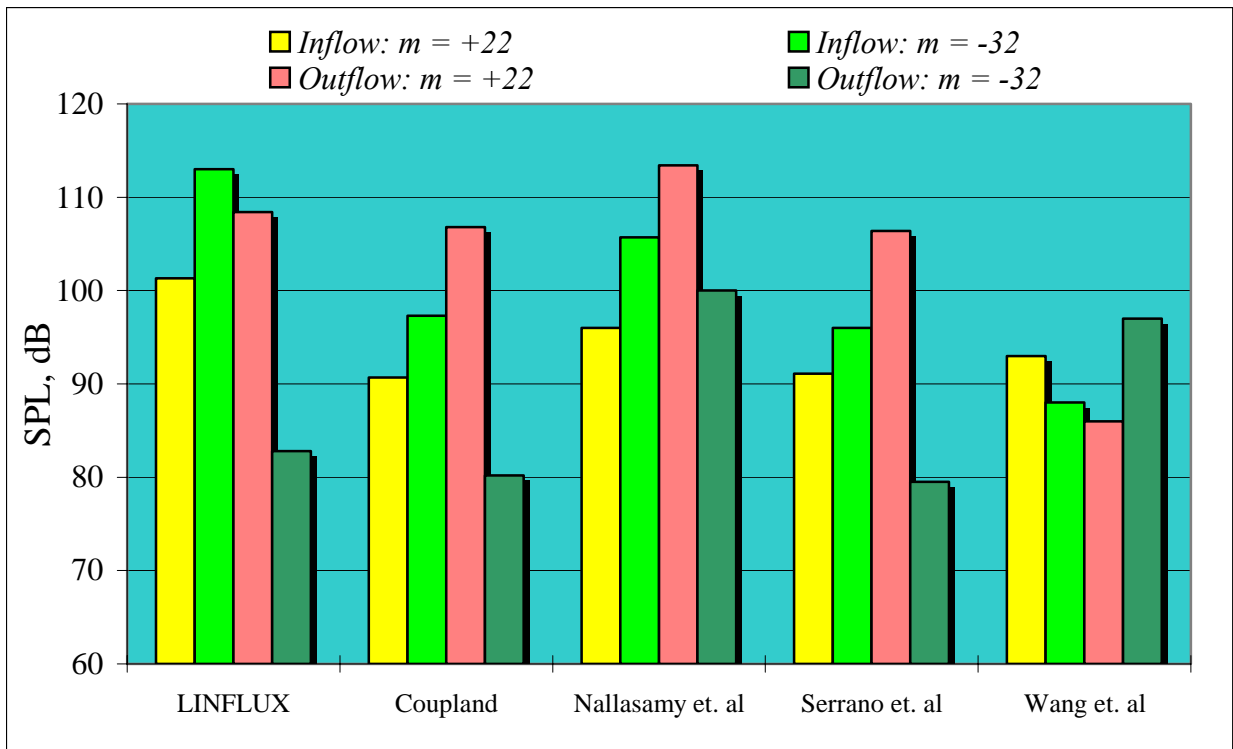


Figure 14. Comparison of computed sound pressure levels at the inflow and outflow planes at frequency ω .

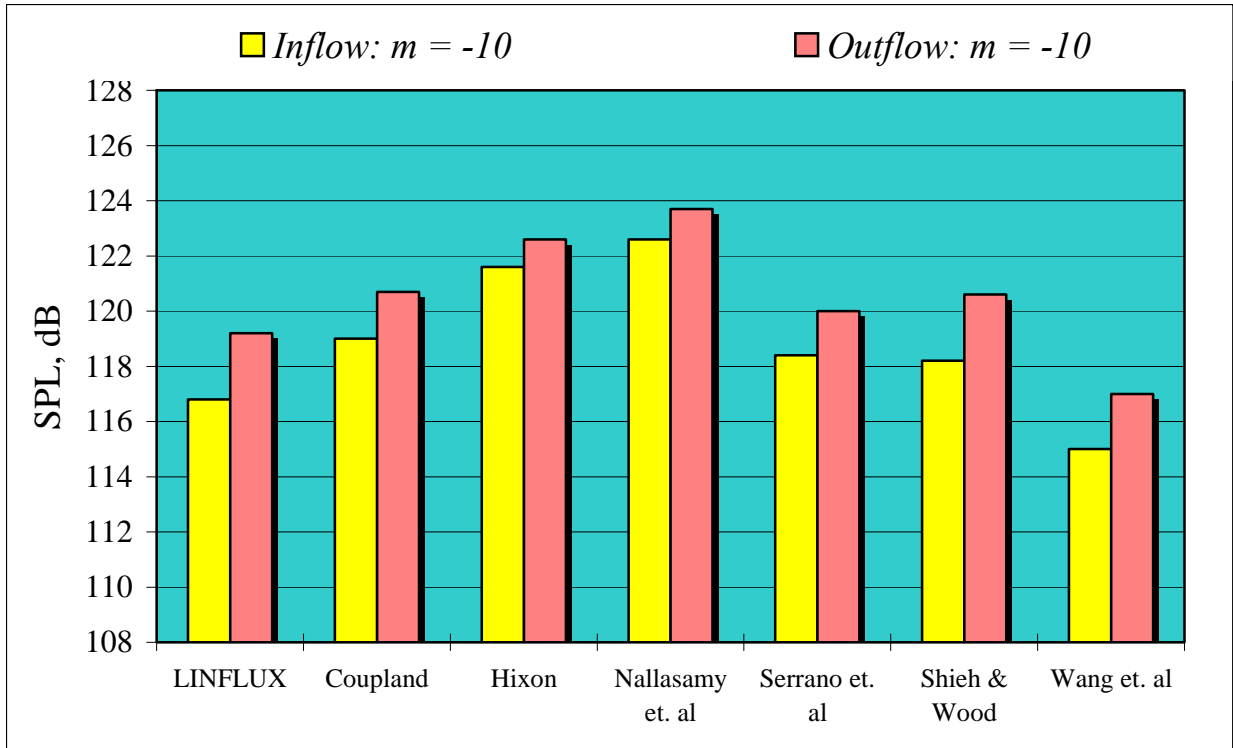


Figure 15. Comparison of computed sound pressure level at the inflow and outflow planes at frequency 2ω .

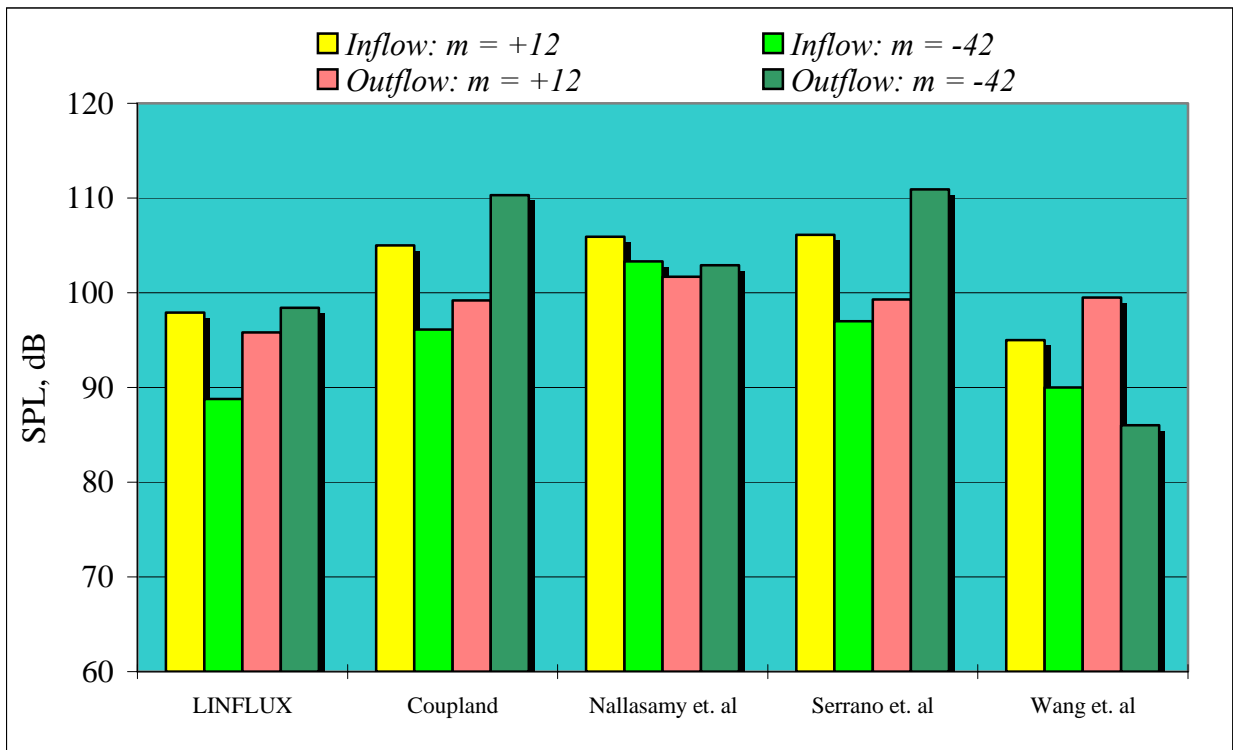


Figure 16. Comparison of computed sound pressure level at the inflow and outflow planes at frequency 3ω .